Autonomous Landing on Ground Target of UAV by Using Image-Based Visual Servo Control

Yongwei Zhang[1], Yangguang Yu[1], Shengde Jia[1], Xiangke Wang[1]

1. College of Mechatronics & Automation, National University of Defense Technology, Changsha 410073, P. R. China
E-mail: zhangyongwei93@163.com
yuyangguang11@nudt.edu.cn
xkwang@nudt.edu.cn

Abstract: This paper addresses the auto landing problem of a quadrotor unmanned aerial vehicle (UAV) equipped with a single down-looking vertically camera on the ground target using image-based visual servo (IBVS) control. Observable features on a ground guidance cooperation mark flat are exploited to recognize and obtain the center pixel position of the mark, without the position and attitude estimation process, and direct compute flight control commands based on pixel level in image by control law, which all running on an onboard micro-processor. We exploited two control schemes include visual velocity landing control and VICON position landing control to compare the control effect. Experimental results are provided to illustrate and assess the performance of the proposed visual control strategy.

Key Words: Unmanned Aerial Vehicle (UAV), Image-Based Visual Servo (IBVS) Control, Automatic Landing, VICON

1 Introduction

The autonomous landing is playing an important role in the auto flight of unmanned aerial vehicles (UAVs), and has attracted considerable attentions in the field of UAVs. In general, the position-based visual servo (PBVS) control, in which the control laws are conducted based on the relative position and attitude between the UAV and the ground landing region, in particular obtaining by the global position system (GPS) or the vision system, is the dominated carried out a vast research [1-3].

In this paper, we mainly pay attention on the autonomous landing by visual servo control scheme, as the camera sensor is mounted cheaply and easily on a UAV currently. A fuzzy control approach was proposed to command the vertical, longitudinal, lateral and orientation velocities of UAV using position-based visual servo control [1]. The pose estimation was based on a vision algorithm with Aruco tag and the IMU equipped by the aerial vehicles. Simulations and experiments with a quadrotor landing in a moving platform are all presented. The authors accomplished onboard the autonomous landing of a UAV using fiducial markers detected by a camera [2], performing state estimation of IMU and Apriltag visual data with a delayed-state extended Kalman filter, and then executing the motion control. In experiments, a motion capture system used for independent ground-truth is presented.

Different to the PBVS, the integration of a visual system in image pixel level directly into the control law design without estimating the relative position and attitude is named image-based visual servo (IBVS) control [4, 5]. Classical image-based visual servo control algorithms were developed in robotic manipulators research field [6], and due to its robustness on errors in target geometry, aerial vehicles field is gaining great interest in developing related visual algorithms [7-9].

A Vertical Take-Off and Landing (VTOL) quadrotor is landing successfully using image based visual servo control in [10]. The proposed control law used only a common sensor suite composing of an onboard camera and IMU sensor, and an optical flow for velocity measurement, and the convergence without estimating any parameter related to the unknown distance is guaranteed. The work continues to advance, with a novel control law proposed to guarantee convergence even in the presence of bounded and possibly time-varying disturbances [11]. To improve performance, the control law includes also an estimator for constant or slowly time-varying, unknown inertial forces.

Dynamic IBVS control with bounded roll and pitch is proposed to control a quadrotor equipped with a downwards facing virtual camera [12]. The proposed control law avoids large roll and pitch angles which would occur when the image feature error is large. The controller is only in a simulation environment.

In this paper, we proposed IBVS control strategy with two different control schemes, achieved autonomous landing on ground target of a quadrotor unmanned aerial vehicle, and compared the control effect in a real environment.

The paper is organized as follows. The model used to design the image-based visual servo (IBVS) control is given in Section 2. Then Section 3 and Section 4 present the algorithm design part of the IBVS and the whole experimental process. Finally, concluding remarks are provided in Section 5.

2 IBVS Model

2.1 Reference Frame

First of all, as shown in Fig. 1, the following coordinate systems are used in this paper.

1) **Pixhawk Frame P:** a NED (North-East-Downward) frame in which the X_P and Y_P axes are aligned with the real north and east magnetic poles of the earth respectively, and the Z_P axis is pointed downward.

2) Body-Fixed ROS Frame N: Onboard processor Odroid XU4 is fixed on the UAV, running ROS (Robot Operating System) with Ubuntu operating system. This frame is an ENU (East-North-Upward) frame in which the X_N and Y_N axes are pointed forward and left of the body respectively, and the Z_N axis is pointed upward. Note that the forward of the body is aligned with the Pixhawk forward arrow.
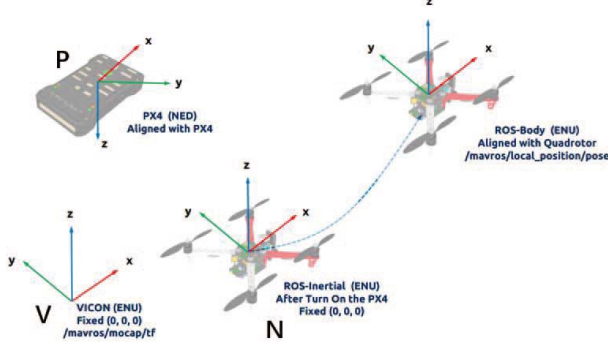

Fig. 1: System frame definition

3) VICON Frame V: This frame is not fixed, as long as it is consistent with the right-hand rule. Taking account of the VICON position and attitude data fuse with the Pixhawk internal sensor accurately, VICON Frame is established align with the Body-Fixed ROS Frame.

4) Camera Frame C: Camera-fixed reference frame that is aligned with the axes of the camera. For simplicity, in the paper camera frame in which the X_C and Y_C axes are aligned with right and backward of the UAV body, and the Z_C axis is pointed downward.

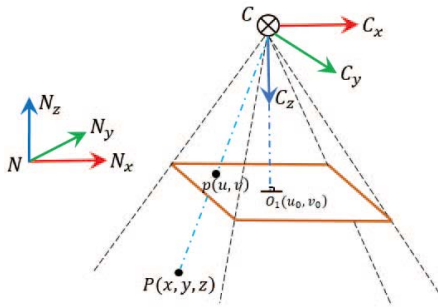**2.2 Camera Perspective Projection**

Fig. 2: Camera perspective projection model

To describe the landing control strategy, two reference frames with camera frame C and body-fixed ROS frame N are introduced as shown in Fig. 2. Also, we assume the camera is attached at the bottom center of the UAV exactly.
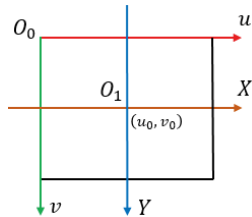

Fig. 3: Camera image frame

Referring to the camera perspective projection model, the image frame is defined first as shown in Fig. 3. (u,v) and (X,Y) are the image frame in pixel and physical unit with O_0 and O_1 as origin, respectively. The physical dimensions of each pixel in the X and Y axis directions are dX and dY, so the coordinates of an arbitrary pixel in image in the two frames have following relationship

$$\begin{cases} u = X/dX + u_0 \\ v = Y/dY + v_0 \end{cases} \quad (1)$$

where (u,v) is the pixel coordinates of a point in image, (u_0, v_0) is the origin coordinates of image frame in pixel.

Converting into homogeneous coordinate and matrix form, equation (1) can be rewritten as following formula

$$\begin{bmatrix} X \\ Y \\ 1 \end{bmatrix} = \begin{bmatrix} dX & 0 & -u_0 dX \\ 0 & dY & -v_0 dY \\ 0 & 0 & 1 \end{bmatrix} \begin{bmatrix} u \\ v \\ 1 \end{bmatrix} \quad (2)$$

The position in the image plane of any spatial point can be approximated by pinhole imaging model, the projection position in the image plane of an arbitrary point P is known as the point where the line OP connecting the optical center O and the point P intersects the image plane, called central projection or perspective projection.

Based on the proportional relationship, the following relation is expressed as

$$\begin{cases} X = fx/z \\ Y = fy/z \end{cases} \quad (3)$$

where (X,Y) is the image coordinates of P, (x,y,z) is the coordinate of spatial point P in the camera frame C.

The perspective projection can transform to the following form

$$s \begin{bmatrix} X \\ Y \\ 1 \end{bmatrix} = \begin{bmatrix} f & 0 & 0 \\ 0 & f & 0 \\ 0 & 0 & 1 \end{bmatrix} \begin{bmatrix} x \\ y \\ z \end{bmatrix} \quad (4)$$

where s is a scale factor.

Based on the formula (2) and (4), we can derive that

$$s \begin{bmatrix} u \\ v \\ 1 \end{bmatrix} = \begin{bmatrix} 1/dX & 0 & u_0 \\ 0 & 1/dY & v_0 \\ 0 & 0 & 1 \end{bmatrix} \begin{bmatrix} f & 0 & 0 \\ 0 & f & 0 \\ 0 & 0 & 1 \end{bmatrix} \begin{bmatrix} x \\ y \\ z \end{bmatrix}$$
$$= \begin{bmatrix} \alpha_x & 0 & u_0 \\ 0 & \alpha_y & v_0 \\ 0 & 0 & 1 \end{bmatrix} \begin{bmatrix} x \\ y \\ z \end{bmatrix} \quad (5)$$

where $\alpha_x = f/dX$, $\alpha_y = f/dY$ are the normalized focal length on the u-axis and v-axis respectively, and $(\alpha_x, \alpha_y, u_0, v_0)$ only relevant to the internal parameters of the camera.

3 Algorithm Analysis

3.1 Landing Overall Design

The overall design of visual servo landing problem of UAV is shown in Fig. 4. A tag plane is fixed at the ground, used for ground guidance landing sign. The aerial vehicle is

11205

equipped with a camera facing the ground. Observable features on the tag plane are exploited to derive a suitable control law to control the UAV landing on the ground steady. At the same time, UAV communicated with the ground computer with control instructions in case of emergency, real-time image and vehicle status information.
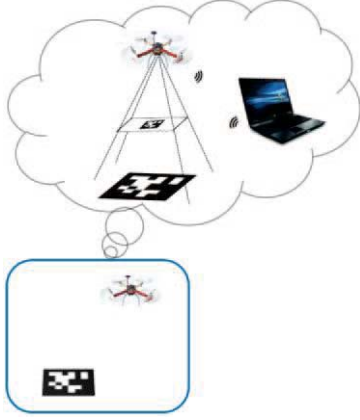

Fig. 4: Overall design of visual servo landing

3.2 Imaging Algorithm Design

The visual velocity control landing software architecture is shown in Fig. 5, the camera facing the ground vertically attached at the bottom center of the UAV collects the real-time image. And then the onboard Odroid board is used to recognize center pixel coordinates of the tag. Based on the center pixel position and the image plane origin position, the velocity control command is obtained, and transmitted to the Pixhawk flight controller. Notice that, although the relative position and orientation of the camera can be obtained from ground cooperation marks, only the pixel level in image is utilized to generate the velocity control command. In fact, a simpler landmark detection algorithm can be used to detect some specific landmarks, such as circular or square combination, whereas the robustness and accuracy of the detection algorithm should take into account seriously. The position and attitude of aerial vehicle from VICON contribute to velocity estimation of UAV and increase flight stability in this scheme.
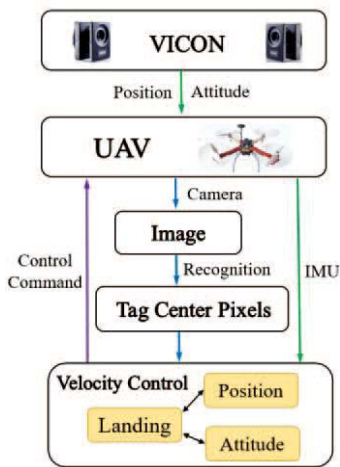

Fig. 5: Visual velocity control landing software architecture

The image processing of tag is shown in Fig. 6. Input of the processing is raw image from camera on UAV, and the output is tag information, including position and attitude between tag and camera equipped on the UAV, and image with mark highlight.
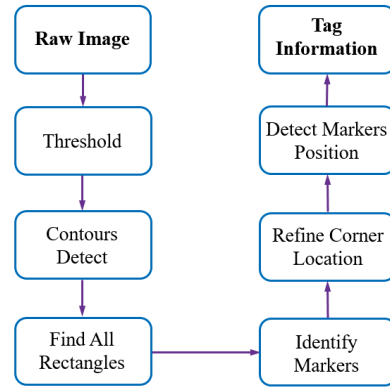

Fig. 6: Image processing of tag

3.3 Control Algorithm Design

Recall equation (5). We assume that the z coordinate of spatial point P is known, and then derive the formula of deviation Δx and Δy in x, y direction between spatial point P and camera frame C as follows

$$\begin{cases} \Delta x = z(u - u_0)/\alpha_x \\ \Delta y = z(v - v_0)/\alpha_y \end{cases} \quad (6)$$

The purpose of the designed controller is prompting Δx and Δy tend to 0.

A PID controller is designed to regulate Δx and Δy converges to zero, that is

$$\begin{cases} U_x(t) = P_x\Delta x(t) + I_x\left[\Delta x(t) + \cdots + \Delta x(0)\right] + D_x\left[\Delta x(t) - \Delta x(t-1)\right] \\ U_y(t) = P_y\Delta y(t) + I_y\left[\Delta y(t) + \cdots + \Delta y(0)\right] + D_y\left[\Delta y(t) - \Delta y(t-1)\right] \end{cases} \quad (7)$$

where (P_x, I_x, D_x), (P_y, I_y, D_y) are PID control parameters in x and y direction , $\Delta x(t), \Delta y(t)$, $\Delta x(t-1), \Delta y(t-1)$, $\Delta x(0), \Delta y(0)$ are the error between spatial point P and camera frame C of current time, previous time and initial time, respectively. $U_x(t)$, $U_y(t)$ are the velocity control of X and Y axis.

Risk usually increase that the closed-loop system will become unstable when introducing feedback. Therefore, stability is a primary requirement in a feedback system. Lots of insight into PID control can be acquired by analyzing the stability region have turns out, which is the set of controller parameters that give stable closed-loop systems.

In this paper, (u, v) and (u_0, v_0) represent the pixel coordinates of the Aruco tag plane center in camera image and the origin of image frame, respectively. And the PID output is 4DOF vector including the velocity control of XYZ axis and Yaw orientation.

4 Experiments

To verified our proposed method, the experiments of a quad-rotor vehicle landing on ground are considered.

4.1 Hardware Setup

A VICON Vantage motion capture system, composing of 24 infrared cameras, together with markers attached to the UAV, is used to provide accurate position and attitude

11206

information of the UAV. VICON Vantage is a high-performance system, which is able to operate with submillimeter and subdegree precision up to 400 HZ. Simultaneously, the linear and angular velocities are well estimated from the position and attitude measurements from VICON Tracker motion capture software.
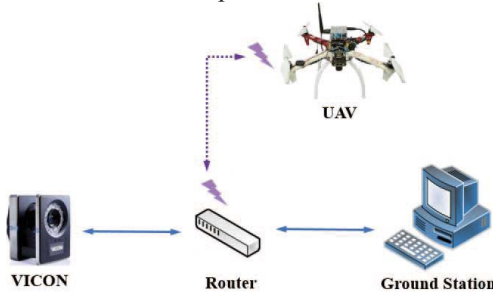

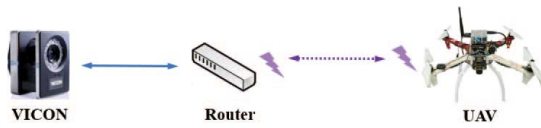Fig. 7: Communication connection scheme 1

Fig. 8: Communication connection scheme 2

Two communication connection schemes are designed for subscribing the VICON data to aerial vehicle, as shown in Fig. 7 and Fig. 8, respectively.

For the first scheme, the VICON Tracker software processes raw data received from VICON cameras, and connects to a router by wired connection. The ground station computer receives position and attitude information processed by Tracker software through the router with wired connection similarly, and send out with ROS topic form by running specific ROS package. And the UAV subscribes the corresponding position and attitude topic from ground station computer with ROS through the router with wireless connection.

For the second scheme as shown in Fig. 8, the UAV directly receives VICON data from Tracker software through the router with wireless connection by running the corresponding specific ROS package.

Compared the two schemes, the first scheme is more complex than the latter seemingly, and the second scheme is more direct and convenient. But the frequency and amount of VICON data are too high processed by Tracker software, so that the wireless connection between UAV and router in the second scheme can't guarantee the data transmission stability. In this paper, the first communication connection scheme is preferred.

Fig. 9: Quadrotor vehicle used in the experimental setup

The vehicle used for the experiments is a quadrotor with DJI F450 airframe, depicted in Fig. 9. The UAV is equipped with a camera vertically facing the ground and an onboard micro-processor Odroid XU4 used for image processing. The image processing result is utilized by the proposed control law to compute flight control commands, which is also running in the micro-processor onboard. Pixhawk flight controller receives the flight control commands from onboard Odroid, to control the flight of UAV. The mark balls attached to the quadrotor are recognized by VICON cameras to compute the precise position and attitude estimations of the UAV. WIFI is used to communication with the ground station computer, and transport images from the camera on quadrotor and keyboard control commands from ground computer.

The onboard micro-processor (quad-core ARM Cortex A15 and quad-core ARM Cortex-A7 highest running at 1.5 GHz) is running Linux operating system and ROS (Robot Operating System). The camera equipped in the UAV is an USB camera with OV2710 sensor, lens size and image area are 1/2.7 inch and $5856\mu m \times 3276\mu m$, respectively. Focal length of the camera lens is adjustable from 2.8mm to 12mm manually with maximum resolution and frame rate up to 1920×1080 and 60fps.

Ground mark is necessary to complete the visual autonomous landing of UAV. Cooperation tag with robustness, stability and practicality is widely used in the unmanned aerial vehicle vision localization. The cooperative two-dimensional codes are usually designed to be detected conveniently, even in the case of partial occlusion and missing or low resolution, in particular, which has four sides, can provide four feature points to be detected is most commonly used, such as AprilTag and Aruco Tag is shown in Fig. 10.

(a) AprilTag   (b) Aruco

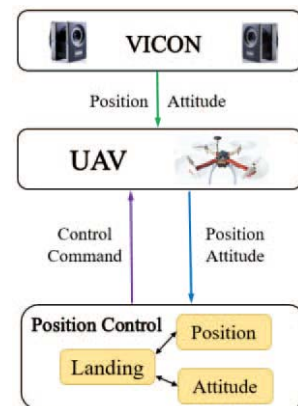Fig. 10: Cooperation marks

4.2 Software Setup

Fig. 11: VICON position control landing software architecture

We exploited two UAV landing schemes by using VICON and visual guidance signs with tag, including UAV velocity

11207

and position control strategy. The visual velocity control landing scheme has shown in Fig. 5. The other scheme software architecture is shown in Fig. 11.

For VICON position control landing scheme, the precise position and attitude data of aerial vehicle are obtained directly from VICON, and then used to generate the position control command. In this strategy, some reflective markers are attached to the target plane in advance, in order to provide ground truth position of the landing spot.

4.3 Experimental Result

The used ground cooperation marks in the paper are AprilTag or Aruco. The recognition algorithm of AprilTag is more complex and stringent than Aruco to ensure the recognition accuracy in a variety of complex environments, maximize prevent the interference from light, resolution, image blur and other factors. But in our application, image processing capacity is limited strongly due to the microprocessor onboard. In experiments, the recognition with AprilTag is only about 10 fps, far from the real-time requirements of the control algorithm. Taking into account both the real-time and accuracy of recognition algorithm, the Aruco tag fulfil our requirements. The image processing can be easily achieved 30 fps and recognition effect is also accurate enough for the UAV flight control.

We tested the Aruco tag recognition algorithm in different environment with light intensity, relative distance and background reflectivity. The recognition results are shown in Fig. 12.
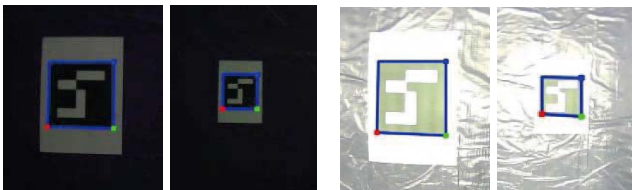

Fig. 12: Aruco recognition results in different environment

The experimental scene performed indoor is shown in Fig. 13. The quadrotor's precise positon is measured by VICON, and the pixhawk can fusion with VICON data to estimate vehicle position accurately through the conversion of the onboard micro-processor. A PID control strategy running on the onboard micro-processor Odroid is applied in this paper, to guarantee the UAV converging to the desired landing spot on the ground.
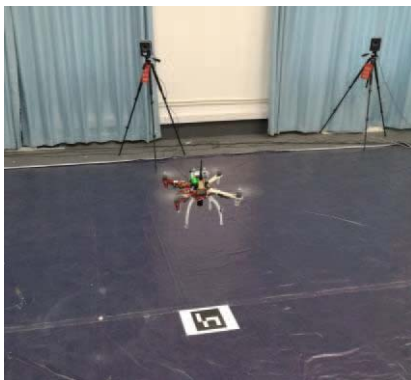

Fig. 13: Experimental scene

We designed two groups of experiments, that are using visual velocity control and VICON position control. The initial landing positions are located in the orientations with 'left forward', 'right forward', 'left backward' and 'right backward' of the ground landing spot. The initial landing altitude in each group of experiments are 1.6m and 2.2m, respectively. The UAV visual velocity control and VICON position control landing experimental results are shown in Fig. 14, Fig. 15 and Fig. 16, Fig. 17, respectively.
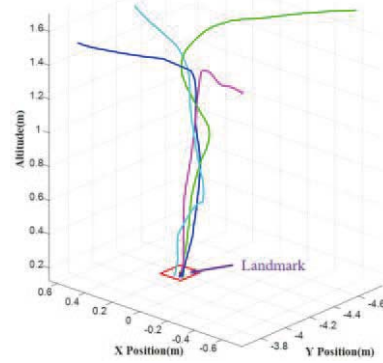

Fig. 14: Visual velocity control landing of four different orientations with initial altitude 1.6m
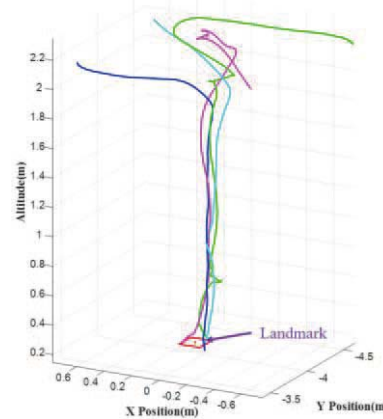

Fig. 15: Visual velocity control landing of four different orientations with initial altitude 2.2m
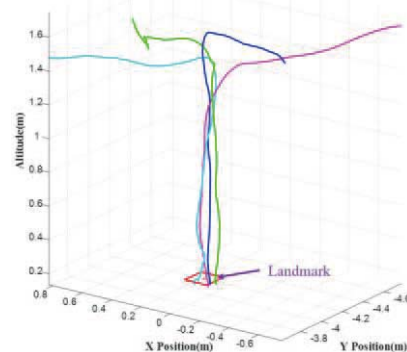

Fig. 16: VICON position control landing of four different orientations with initial altitude 1.6m
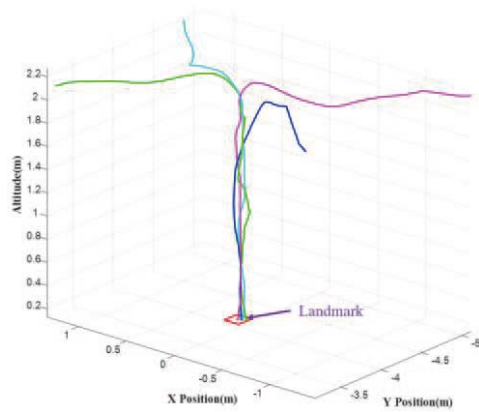
11208

Fig. 17: VICON position control landing of four different orientations with initial altitude 2.2m

The experiments show that, the proposed visual velocity control and the VICON position control with different initial landing altitude and orientations relative to the ground landing spot are able to convergence to the desired landing spot on the ground.

For visual velocity control, in the initial and final landing phase, the cases with initial altitude 1.6m are more stable with less overshoot and more accurately landing on the landmark than the that with initial altitude 2.2m. But in the landing process, the cases with initial altitude 2.2m are more stable with less shaking in horizontal plane. In some experiments, the landing process performed almost wonderful, which evidence the visual guidance landing strategy of Aruco tag with pixel level in image is feasible, and the PID parameters are available but also need to be fine tuning carefully.

The landing process with VICON position control can be considered as a standard process base on the precise position and attitude estimations, and the experimental results proved the effectiveness of the landing control strategy.
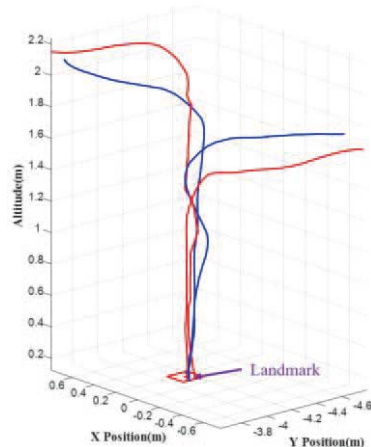

Fig. 18: Two control strategies comparison (red: VICON position control blue: visual velocity control)

In order to compare the landing control effects of the two control strategies, only two groups of experiments with different initial landing altitude are shown in Fig. 18.

From the comparison, we can infer that the proposed visual velocity control strategy is completely feasible and the convergence of control law is proven by practices.

5   Conclusions

This paper addresses the landing problem of a quadrotor unmanned aerial vehicle on ground target using image-based visual servo control. The proposed visual control strategy uses only the center pixel position of the ground guidance cooperation mark, which is provided from an onboard camera and recognized by the onboard micro-processor. The pixel level in image is used in a way that allow direct compute and generates flight control commands without the requirements of estimating position and attitude of UAV.

Compared with the visual velocity control and VICON position control schemes, the effectiveness and feasibility of the visual control scheme are verified by a mount of experimental results.

References

[1]   Olivares-Mendez M A, Kannan S, Voos H, Vision based fuzzy control autonomous landing with UAVs: From V-REP to real experiments, *Control and Automation (MED), 2015 23th Mediterranean Conference on. IEEE*, 2015: 14-21.

[2]   Chaves S M, Wolcott R W, Eustice R M, NEEC Research: Toward GPS-denied Landing of Unmanned Aerial Vehicles on Ships at Sea[J]. *Naval Engineers Journal*, 2015, 127(1): 23-35.

[3]   Yang S, Ying J, Lu Y, et al, Precise quadrotor autonomous landing with SRUKF vision perception[C], *2015 IEEE International Conference on Robotics and Automation (ICRA). IEEE*, 2015: 2196-2201.

[4]   Chaumette F, Hutchinson S, Visual servo control. I. Basic approaches[J], *IEEE Robotics & Automation Magazine*, 2006, 13(4): 82-90.

[5]   Chaumette F, Hutchinson S, Visual servo control. II. Advanced approaches [Tutorial][J], *IEEE Robotics & Automation Magazine*, 2007, 14(1): 109-118.

[6]   Gangloff J A, de Mathelin M F, Visual servoing of a 6-DOF manipulator for unknown 3-D profile following[J], *IEEE Transactions on Robotics and Automation*, 2002, 18(4): 511-520.

[7]   Serra P, Cunha R, Silvestre C, et al, Visual servo aircraft control for tracking parallel curves[C], *2012 IEEE 51st IEEE Conference on Decision and Control (CDC). IEEE*, 2012: 1148-1153.

[8]   Serra P, Le Bras F, Hamel T, et al, Nonlinear IBVS controller for the flare maneuver of fixed-wing aircraft using optical flow[C], *49th IEEE Conference on Decision and Control (CDC). IEEE*, 2010: 1656-1661.

[9]   Chavez A, L'Heureux D, et al, Homography-Based State Estimation for Autonomous UAV Landing[M], *AIAA Information Systems-AIAA Infotech@ Aerospace.* 2017: 0673.

[10] Serra P, Cunha R, Hamel T, et al, Landing on a moving target using image-based visual servo control[C], *53rd IEEE Conference on Decision and Control. IEEE*, 2014: 2179-2184.

[11] Serra P, Cunha R, Hamel T, et al, Landing of a Quadrotor on a Moving Target Using Dynamic Image-Based Visual Servo Control[J], *IEEE Transactions on Robotics*, 2016, 32(6): 1524-1535.

[12] Xie H, Lynch A, Dynamic image-based visual servoing for unmanned aerial vehicles with bounded inputs[C], *Electrical and Computer Engineering (CCECE), 2016 IEEE Canadian Conference on. IEEE*, 2016: 1-5.